

OBSERVATIONS OF CAVITATION ON A THREE-DIMENSIONAL OSCILLATING HYDROFOIL

D. P. Hart, C. E. Brennen, and A. J. Acosta
California Institute of Technology
Pasadena, California

Abstract

A test apparatus was designed and constructed to observe the effect of sinusoidal pitching oscillations on the cavitation of three-dimensional hydrofoils. The apparatus is capable of oscillating hydrofoils at a rate up to 50 Hz and provides for adjustments in oscillation amplitude and mean angle of attack. Observations of the effect of pitching oscillation on cavitation have been made for a NACA 64-309 (modified) hydrofoil operating at its designed mean angle of attack of 7° with an oscillation amplitude of 2° . Photographs illustrating the interaction between natural cavity shedding frequencies and the foil reduced frequency are included.

Nomenclature

- c = Foil chord length, 0.154m (6in)
- f = Excitation frequency in Hz
- k = Reduced frequency = $\omega c/2U_\infty$
- P_v = Water vapor pressure in kPa
- P_∞ = LTWT test section pressure in kPa
- Re = Reynolds number = $U_\infty c/\nu$
- U_∞ = LTWT test section velocity in m/s
- ω = Foil excitation frequency in rad/s
- α = Hydrofoil angle of attack in degrees
- ν = Kinematic viscosity in m^2/s
- ρ = Fluid density in kg/m^3
- σ = Cavitation number = $(P_\infty - P_v)/(0.5\rho U_\infty^2)$

1. Introduction

Oscillating foils provide a convenient means of simulating the effects of freestream velocity fluctuations on cavitation. These fluctuations have a pronounced influence on the performance of propellers, hydrofoils and turbomachinery. It affects not only the inception of cavitation but also the form in which cavitation appears (Avellan et. al. [1989]). A number of theoretical, numerical, and experimental studies have been devoted to the subject of oscillating foils. However, these investigations deal primarily with two-dimensional foils whereas the study of three-dimensional oscillating foils have, in the past, re-

ceived very little attention. In an effort to explore this area, we recently constructed a test apparatus to oscillate three-dimensional hydrofoils in the Low Turbulence Water Tunnel (LTWT) (Gates [1977]).

2. Experimental Setup

The oscillating foil mechanism, shown in Figure 1, was designed and constructed to mount to the underneath side of the working section of the LTWT. When in place, this mechanism is capable of pitching a hydrofoil in a sinusoidal fashion at a rate variable from 0 to 50 Hz. It is driven by a one horsepower DC motor coupled to the hydrofoil by a three bar linkage. A slip collet at the hydrofoil end of this linkage allows the hydrofoil mean angle of attack to be adjusted. The hydrofoil itself mounts to an aluminum plate recessed in the floor of the LTWT test section. It pivots about a stainless steel shaft mounted 0.38c from the leading edge of the foil. The phase angle and oscillation rate of the hydrofoil are monitored by an optical shaft encoder mounted on the DC motor. The encoder output, 1024 pulses per cycle, is supplied to a digital tachometer and to a synchronizer which allows instrumentation to be synchronized with the foil position. The oscillation rate is controlled in an open loop fashion by a Sabina motor control unit.

The LTWT is capable of operating at speeds up to 10 m/s and pressures down to 18 kpa. A Zenith 120 microcomputer has been adapted to continuously monitor the tunnel operating conditions including velocity, pressure, and temperature.

Photographs of the hydrofoil cavitation were taken using two Strobotac 1531-A strobe lights mounted to the top of the LTWT test section. The camera shutter was opened and a single flash was triggered at a chosen moment during an oscillation cycle using the output from the motor shaft encoder. The 10 microsecond flash duration of the strobes in combination with Konica 3200 ASA film allowed the cavitation events to be captured clearly.

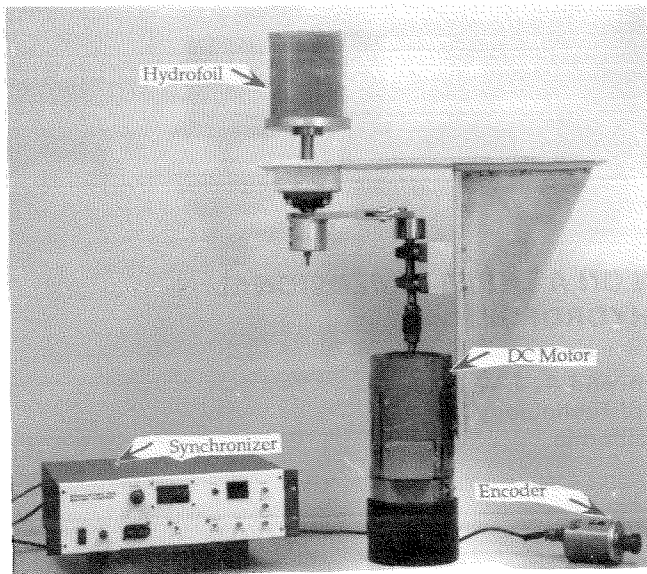


Figure 1. Oscillating Foil Mechanism.

3. Observation and Discussion

The present paper will describe preliminary observations made of cavitation on a reflection-plane mounted, aspect 2.3, NACA 64-309 (modified) hydrofoil oscillating in a sinusoidal fashion with an amplitude of 2° at the design mean angle of attack of 7° . Comparisons are made for reduced frequencies, k , from 0.15 to 1.5, Reynolds numbers, Re , ranging from 11×10^5 to 13×10^5 and a dissolved air content of 6 ppm. In all cases, cavitation inception was first observed in the tip vortex about three chords downstream from the trailing edge and occurred at a cavitation inception number, σ , of about 2.1. This cavitation then moved upstream as the tunnel pressure was decreased until it attached to the foil tip on the suction side near the trailing edge. Leading edge cavitation did not appear until the cavitation number was approximately half that of tip vortex cavitation inception, about $\sigma \approx 1.0$.

Leading edge cavitation first appears on the suction side of the hydrofoil as traveling bubble cavitation which, as the cavitation number is reduced, quickly becomes attached cavitation near the base of the foil. With further reduction, the attached cavitation grows from the base outward towards the tip. The trailing edge of this attached cavity has a parabolic shape which follows the pressure contour characteristic of finite aspect ratio foils. At the base of the hydrofoil, where the attached cavity initially forms, there is a strong interaction between the hydrofoil and the tunnel boundary layer. The result of this interaction is an increased pressure which suppresses cavitation near the mid-chord and trailing edge of the foil. When the leading edge cavity collapses (due to the natural shedding frequency of the cavitation, the oscillation of the foil or a combination of both), a bubbly cloud near the base of the hydrofoil is formed. A ring vortex often emerges from the downstream side of this cloud and the cloud and vortex dissipate several chords downstream of the trailing edge.

We now examine the response of the cavitation to the hydrofoil oscillation between angles of attack of 5° and 9° . In general, the leading edge cavitation forms and collapses with

the oscillation of the hydrofoil. However, there exists a phase lag between the extent of the leading edge cavitation and the foil oscillation which tends to increase with increased frequency. At lower reduced frequencies, leading edge cavitation forms and grows an appreciable amount before the hydrofoil has reached its maximum angle of attack. The cavitation then remains until the hydrofoil angle of attack is well below that at which inception occurs. At the higher reduced foil frequencies of 0.3 or greater, leading edge cavitation does not grow significantly until after the hydrofoil has reached its maximum oscillation amplitude. Again, it remains until the hydrofoil angle of attack is well below the point of inception.

In addition to the noticeable phase lag between the hydrofoil and the cavitation oscillations, a strong interaction between the hydrofoil reduced frequency and the natural shedding frequency of the leading edge cavitation exists. Cavitation on the leading edge of the foil sheds and reforms at a frequency not only dependent on the excitation frequency but also on the Reynolds number of the flow. The photographs in Figures 2 through 4 illustrate this interaction between the natural shedding frequency and the excitation frequency. They show the suction side of the hydrofoil with rounded tip operating at a Reynolds number of 12×10^5 and a cavitation number of 0.5 as it oscillates from 9° to 5° in 0.5° increments. Figure 2 shows the hydrofoil at a reduced frequency of 0.35 or an oscillation rate of 6 Hz which is slightly below the 8 Hz cavity shedding frequency observed when the hydrofoil is held stationary at 7° angle of attack. Notice the two distinct cavities that exist at 7.5° angle of attack and the ring vortex that remains from a previous cavity collapse. As the excitation frequency is increased to 8 Hz (Figure 3) two separate collapses no longer occur. Observations at this frequency reveal that the points of cavitation formation and collapse during an oscillation cycle are very inconsistent. At a higher excitation frequency of 12 Hz (Figure 4) the cavity formation and collapse remain very similar to that at 8 Hz but the points during the oscillation

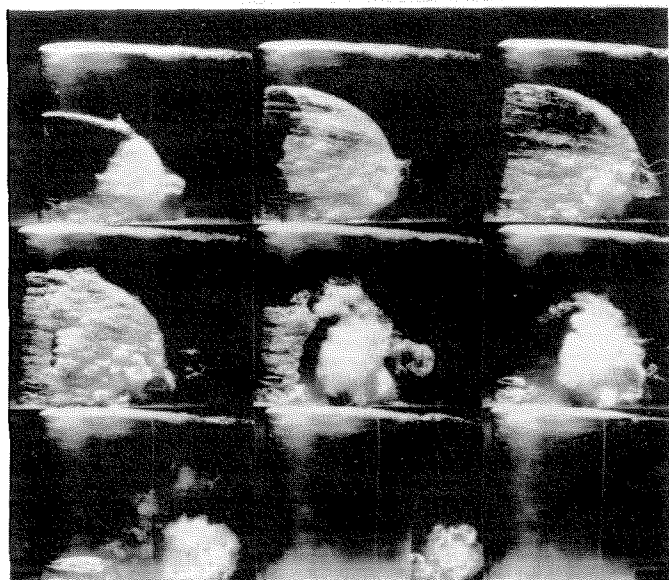


Figure 2. Leading Edge Cavitation ($Re = 12 \times 10^5$, $\sigma = 0.5$, $k = 0.44$).

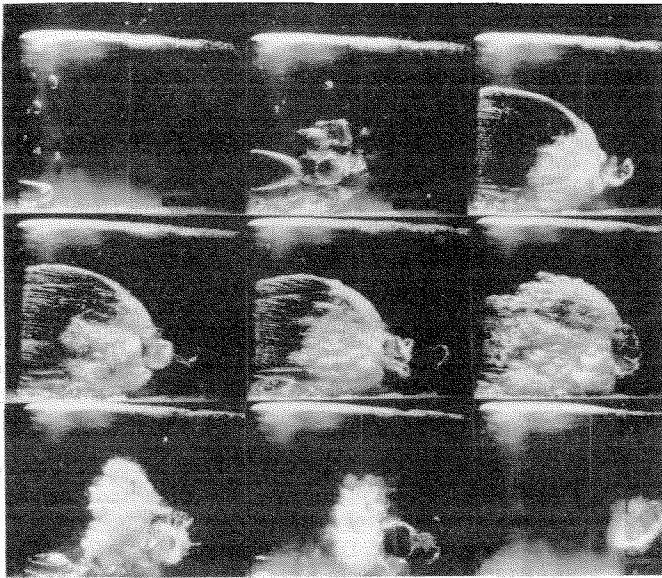


Figure 3. Leading Edge Cavitation ($Re = 12 \times 10^5$, $\sigma = 0.5, k = 0.57$).

cycle at which they occur have now become quite consistent. Unlike the 6 Hz excitation case both the 8 Hz and the 12 Hz excitation cases result in a loud pounding sound as the cavities collapse. Note the phase lag between the hydrofoil angle of attack and the extent of cavitation that exists in all three sets of photographs.

As one would expect, oscillating the hydrofoil significantly affects the cavitation number at which inception occurs. Figure 5 illustrates this by showing the leading edge cavitation inception index as a function of hydrofoil phase angle for reduced frequencies, k , ranging from 0.22 to 1.82. The hydrofoil phase angle shown in this figure corresponds to an angle of attack of 5° at a phase angle of 0° increasing to 9° at a phase angle of 180° and then decreasing back to 5° at a phase angle of 360° . Note that as the excitation frequency is increased a phase shift develops and results in the largest cavitation inception index occurring later in the oscillation cycle. Moreover, even at an excitation frequency of 4 Hz a significant asymmetry occurs in inception. This phenomena is better illustrated in Figure 6. Here the data has been plotted in the form of a hysteresis diagram with the lower traces representing an increasing angle of attack and the upper traces representing a decreasing angle of attack. As the excitation frequency increases, there is an increased hysteresis between cavitation inception and desinence. This hysteresis, however, is largely due to kinematic effects which result in a difference between the hydrodynamic angle of attack of the leading edge moving relative to the freestream flow and the geometric angle of attack of the hydrofoil relative to the tunnel floor. When the data is plotted relative to the hydrodynamic angle of attack (Figure 7.), it collapses to an extent which suggests a universal relationship between inception and the instantaneous hydrodynamic angle of attack. Stationary surface cavitation inception index for this foil as a function of angle of attack was documented by Green [1988] and is included for comparison. The reason for the discrepancy between this data and that of Green is unknown at the present time.

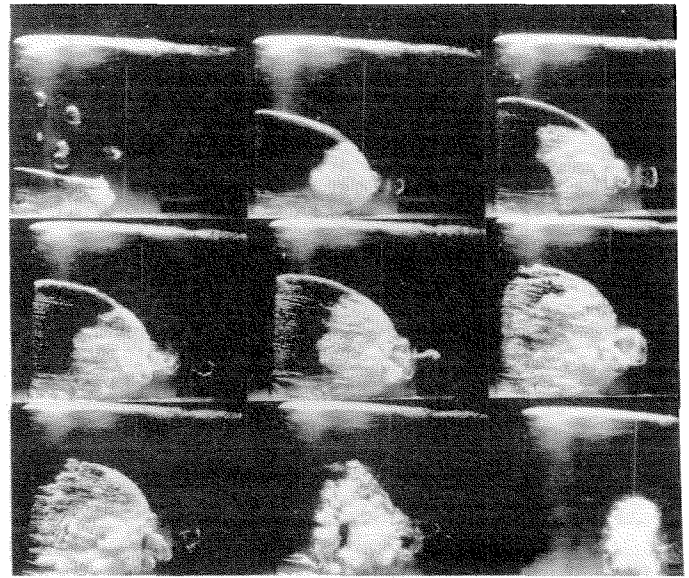


Figure 4. Leading Edge Cavitation ($Re = 12 \times 10^5$, $\sigma = 0.5, k = 0.88$).

4. Conclusions

The effect that freestream velocity fluctuations have on the cavitation of a hydrofoil of finite aspect ratio has been investigated using a test facility designed to pitch a hydrofoil in a sinusoidal fashion about its center of pressure. Photographs taken with strobes synchronized to the hydrofoil motion show that there is a dependence of the observed cavitation formation and inception on the hydrofoil reduced frequency. Furthermore, observations indicate that there can be a strong interaction between the natural shedding frequency of the leading

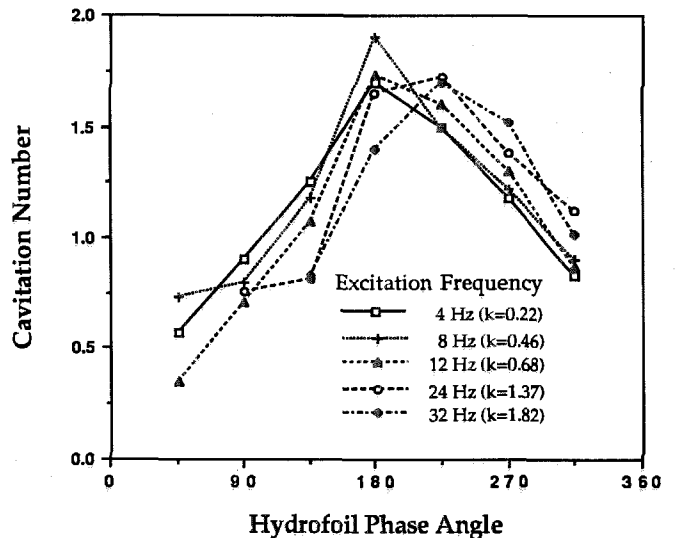


Figure 5. Leading Edge Cavitation ($Re = 12 \times 10^5$). The maximum and minimum angles of attack correspond to phase angles of 180° and 0° (or 360°) respectively.

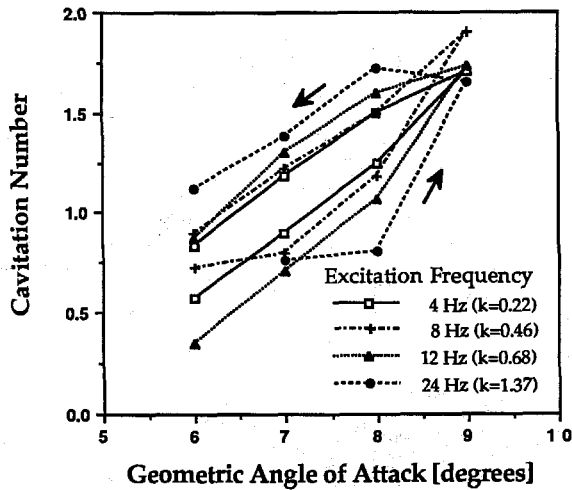


Figure 6. Leading Edge Cavitation as a Function of Hydrofoil Geometric Angle ($Re = 12 \times 10^5$).

edge cavitation and the hydrofoil excitation frequency leading to irregular cavitation patterns and violent cavity collapses. However, investigations of leading edge cavitation inception indicates that within the range of reduced frequencies investigated, the increase in the cavitation number at which inception occurs is primarily due to the increase in hydrodynamic angle of attack resulting from the kinematics of the oscillating foil.

5. Acknowledgments

The authors are grateful for the support of the Office of Naval Research under grant number N00167-85-K-0165. We should also like to thank Professor S. Green at the University of British Columbia for his help in initiating this project and S. Ceccio for his continuing support.

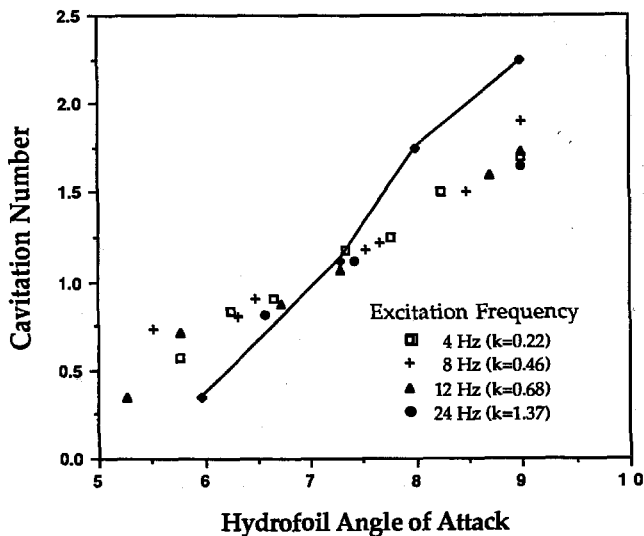


Figure 7. Leading Edge Cavitation as a Function of Hydrofoil Hydrodynamic Angle of Attack ($Re = 12 \times 10^5$). The Solid line represents stationary leading edge cavitation data from Green [1988].

6. References

- Avellan, F., Dupont, P., Ryhming, I. 1989. Generation Mechanism and Dynamics of Cavitation Downstream of a Fixed Leading Edge Cavity Proc. of 17th Symposium on Naval Hydrodynamics, National Academy Press, Washington D.C., pp. 317-329.
- Avellan, F., Farhat, M. 1989. Shock Pressure Generated by Cavitation Vortex Collapse, Proc. of Int. Symp. on Cav. Noise and Erosion in Fluid Mech., San Francisco, pp. 119-125.
- Bartels, F. 1989. Model Tests on Noise Characteristics of Propeller Cavitation in Wake Flow, Proc. of Int. Symp. on Cav. Noise and Erosion in Fluid Mech., San Francisco, pp. 47-54.
- Gates, E. M. 1977. The Influence of Freestream Turbulence, Freestream Nuclei Populations, and Drag-Reducing Polymer on Cavitation Inception on Two Ansymmetric Bodies. Calif. Inst. of Tech., Div. of Eng. and Appl. Sci., Report No. E182-2.
- Green, S. I. 1988. Tip Vortices - Single Phase and Cavitating Flow Phenomena Ph.D. Thesis, Calif. Inst. of Tech. Div. of Eng. and Appl. Sci., Report No. 183-17.
- Kato, H., Ye, Y. P., and Maeda, M. 1989. Cavitation Erosion and Noise Study on a Foil Section. Proc. of Int. Symp. on Cav. Noise and Erosion in Fluid Mech., San Francisco, pp. 79-88.